

www.acsabm.org Article

Identification of TrkB Binders from Complex Matrices Using a Magnetic Drug Screening Nanoplatform

Zekiye Ceren Arituluk, Jesse Horne, Bishnu Adhikari, Jeffrey Steltzner, Shomit Mansur, Parmanand Ahirwar, Sadanandan E. Velu, Nora E. Gray, Lukasz M. Ciesla,* and Yuping Bao*



Cite This: ACS Appl. Bio Mater. 2021, 4, 6244–6255



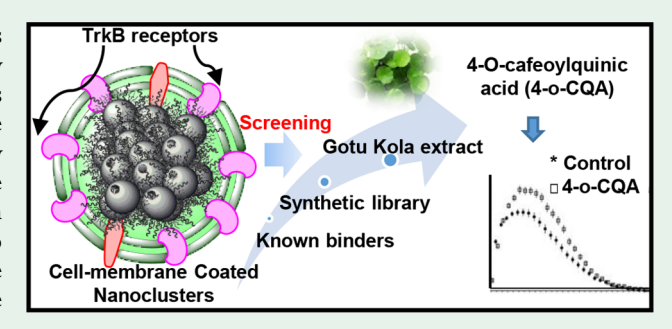
ACCESS

III Metrics & More



SI Supporting Information

ABSTRACT: Brain-derived neurotrophic factor (BDNF) and its receptor tyrosine receptor kinase B (TrkB) have been shown to play an important role in numerous neurological disorders, such as Alzheimer's disease. The identification of biologically active compounds interacting with TrkB serves as a drug discovery strategy to identify drug leads for neurological disorders. Here, we report effective immobilization of functional TrkB on magnetic iron oxide nanoclusters, where TrkB receptors behave as "smart baits" to bind compounds from mixtures and magnetic nanoclusters enable rapid isolation through magnetic separation. The presence of the immobilized TrkB was confirmed by specific antibody labeling.



Subsequently, the activity of the TrkB on iron oxide nanoclusters was evaluated with ATP/ADP conversion experiments using a known TrkB agonist. The immobilized TrkB receptors can effectively identify binders from mixtures containing known binders, synthetic small molecule mixtures, and Gotu Kola (*Centella asiatica*) plant extracts. The identified compounds were analyzed by an ultrahigh-performance liquid chromatography system coupled with a quadrupole time-of-flight mass spectrometer. Importantly, some of the identified TrkB binders from Gotu Kola plant extracts matched with compounds previously linked to neuroprotective effects observed for a Gotu Kola extract approved for use in a clinical trial. Our studies suggest that the possible therapeutic effects of the Gotu Kola plant extract in dementia treatment, at least partially, might be associated with compounds interacting with TrkB. The unique feature of this approach is its ability to fast screen potential drug leads using less explored transmembrane targets. This platform works as a drug-screening funnel at early stages of the drug discovery pipeline. Therefore, our approach will not only greatly benefit drug discovery processes using transmembrane proteins as targets but also allow for evaluation and validation of cellular pathways targeted by drug leads.

KEYWORDS: BDNF/TrkB, drug discovery, receptor immobilization, magnetic nanoclusters, plant extract, neurologic disorders

■ INTRODUCTION

The treatment of neurodegenerative diseases remains as a great medical challenge, which affects millions of people, such as Alzheimer's disease (AD), Parkinson's disease (PD), and many other neurological disorders. Currently, truly effective treatments for neurodegenerative diseases are not available.^{2,3} For example, clinical translation of nearly all (>400) tested compounds for AD were unsuccessful, where all the compounds were developed relying on the amyloid beta plaque hypothesis.4 Therefore, there is an urgent need to develop approaches allowing for the identification of compounds interacting with and modulating novel and less explored targets. Alternative approaches of developing neuroprotective therapies to activate and restore neuronal functions have recently attracted much attention.^{2,5} For instance, many studies have shown that low levels of brain-derived neurotrophic factor (BDNF) and dysregulation of BDNF high affinity receptor tropomyosin-receptor-kinase B (TrkB) are associated with neurological disorders, such as AD.6-9 For

example, BDNF, the physiological TrkB activator, was found to have protective effects, both in *in vitro* and *in vivo*, on $A\beta$ induced neurotoxicity. BDNF administration directly to rat brain was shown to increase learning and memory in impaired animals. Unfortunately, BDNF cannot be used as a treatment option because of its poor bioavailability, inability to penetrate the blood brain barrier, and the observed adverse side effects from its oral administration. Alternative approaches using small molecule activators to stimulate TrkB have been explored. For instance, 7,8-dihydroxyflavone (7,8-DHF), a natural molecule in the family of flavonoids, was shown to activate TrkB. These studies suggested that TrkB might

Received: May 12, 2021 Accepted: July 11, 2021 Published: July 26, 2021





ACS Applied Bio Materials www.acsabm.org Article

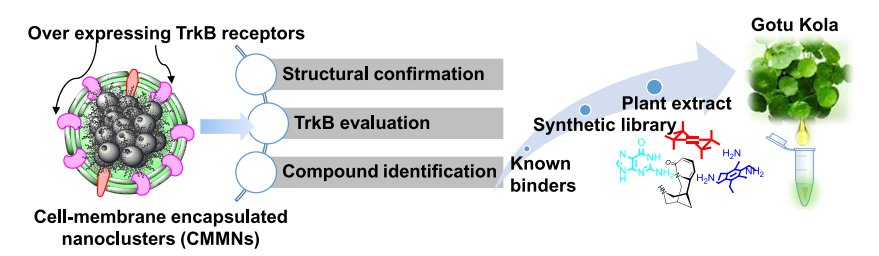


Figure 1. Schematic overview of reported studies: CMMN structure, characterization, and screening experiments.

serve as a valid target for neurological and psychiatric disorders. ^{9,15} In fact, a derivative of 7,8-DHF is currently under consideration as a possible drug for AD. ¹⁶ In addition, it has been shown that the mimetics of TrkB binding domains (loop II) of BDNF, such as LM22A compounds, directly activated TrkB, exhibiting neurotrophic activity. ¹⁷ Peptides mimicking BDNF on nanostructure surfaces were also shown to activate the TrkB signaling pathway. ¹⁸

In addition to the role in neurological disorders, BDNF/ TrkB pathway was shown to be involved in tumor growth and metastasis for several cancer types, such as breast, lung, and neuroblastoma. 19–22 In particular, activation or inhibition of TrkB led to distinct cancer responses. For example, activation of TrkB was shown to decrease the sensitivity of cancer cells to chemotherapy drugs, resulting in drug resistance and enhanced cancer metastasis. On the other hand, inhibition of TrkB showed effectiveness in preventing cancer metastasis and progression. 19,24 Several small molecule drugs have been FDA approved to treat cancer by targeting kinase receptors, such as entrectinib approved in August, 2019 and larotrectinib approved in November, 2018. Therefore, identification of TrkB specific binders (activators or inhibitors) is of great medical importance for both neurological disorders and cancer treatment.

TrkB is a transmembrane protein that stimulates a number of biological pathways upon activation. The use of transmembrane receptors as pharmacological targets is significant, because more than 50% of all modern drugs target transmembrane proteins.^{25–27} Identification of small molecules targeting transmembrane receptors is particularly challenging in drug discovery because these proteins require boundary lipids to function. In order to identify binding compounds targeting TrkB, compounds are typically tested using traditional cell-based assays. ^{28–30} One of the major limitations of this method is that it allows for only screening individual compounds but not mixtures, which precludes the use of complex matrices such as plant/bacterial/fungal extracts or synthetic mixtures. In addition, cellular processes always are associated with many different pathways, which makes it difficult to elucidate the specific biological process involved. Therefore, it is highly desirable to design a screening platform allowing for screening complex mixtures for direct identification of TrkB binding compounds. Traditional screening methods often require isolation of individual compounds from mixtures through chemical separation, followed by dereplication and assay analysis, which are time-consuming, laborintensive, and costly. 31 High throughput screening techniques mainly focus on synthetic libraries of individual compounds and are not compatible with mixtures.³² Immobilization of transmembrane proteins on solid surfaces has been previously studied for the identification of drug candidates from complex

natural matrices, but maintaining receptor activity has been challenging. $^{28,29,33-36}$

While several other techniques of protein immobilization have been reported, several aspects of these approaches are not suitable for immobilizing transmembrane receptors and screening complex mixtures. For example, magnetic bead technology can directly fish out binding compounds through the immobilized protein targets on the bead surfaces, eliminating the need to isolate individual compounds. 28,37 However, the immobilized proteins have been limited to cytosolic proteins, 28 such as enzymes 38 and antibodies. 28,39 This is a significant limitation, because over 50% of all modern pharmaceuticals use membrane proteins as prime targets.^{25–27} In addition, magnetic bead separation suffers from significant nonspecific binding of compounds to the bead surfaces, making them unsuitable for screening complex matrices.²⁸ Another approach, known as cellular membrane affinity chromatography, attempts to immobilize cell membrane fragments on micron-sized silica beads as the stationary phase in packed columns for compound fishing.²⁹ However, the preparation of the packed column requires a large amount of cells and is time-consuming.⁴⁰ In addition, the use of high pressure during the stationary-phase packing process causes protein activity loss, 41 leading to a short column lifespan. 41 We have demonstrated the proof of concept using cell membranecoated iron oxide nanoparticles to screening mixtures, 42 where the immobilized nicotinic receptors behaved as "smart baits" to bind compounds from mixtures and magnetic nanoparticles enabled rapid isolation through magnetic separation. However, the encapsulation of different amounts of nanoparticles inside cell membranes leads to different sizes of nanostructures and an inhomogeneous magnetic response.

In this paper, we report the immobilization of a novel target for neurological disorders, functional TrkB receptors on magnetic iron oxide nanoclusters (a cluster of iron oxide nanoparticles). Here, iron oxide nanoclusters are fully encapsulated inside cell membranes with functional TrkB receptors. The presence of TrkB receptors was confirmed with fluorescence specific antibody labeling, and their activities were evaluated with ATP/ADP conversion experiments. Subsequently, TrkB receptors on nanocluster surfaces were used as targets to identify TrkB binders from compound mixtures with three levels of complexity: mixtures with known binders of known concentrations, a synthetic small molecule library, and plant extracts. To exclude nonspecific binding, a nanoplatform was also prepared using a parental cell line not expressing TrkB receptors as the negative control for all experiments. Compounds binding to the drug-screening platform prepared with the TrkB-expressing cell line and not binding to those obtained from TrkB-null cell line were marked as binders. Compounds binding to the nanoplatform prepared with both types of cells were marked as nonspecific binders.

A schematic overview of the reported studies is shown in Figure 1, where the drug discovery assay based on cellmembrane encapsulated magnetic nanoclusters (CMMNs) was first confirmed structurally with functional TrkB and then was applied to screen an artificial mixture with a known binder, a synthetic small molecule library, and Gotu Kola plant extracts. This assay allows for directly fishing out TrkB binders from very complex matrices. Importantly, some of the identified compounds from Gotu Kola plant extracts agreed well with previously reported compounds from an extract currently used in a clinical trial. Our studies suggested that the possible therapeutic effects of the Gotu Kola plant extract in dementia treatment, at least partially, might be associated with compounds interacting with TrkB. Therefore, our approach will not only greatly benefit the drug discovery process using transmembrane protein as targets but also allow for the evaluation and validation of cellular pathways of the tested molecules.

■ RESULTS AND DISCUSSION

This paper developed a drug-screening platform, CMMNs with functional TrkB receptors. TrkB is an integral transmembrane protein, where the presence of the preserved boundary lipids is critical to maintaining TrkB functions. Therefore, cell membrane fragments rather than free purified TrkB proteins were first prepared and subsequently used to encapsulate iron oxide nanoclusters.

Preparation and Characterization of CMMNs with TrkB Receptors. The cell membrane fragments with TrkB were prepared using SH-SY5Y neuroblastoma cells overexpressing TrkB following our previously developed protocols with slight modification. Numerous protocols on the preparation of cell membrane fragments have been reported prior to their immobilization on solid surfaces.²⁸ We have tested several experimental conditions and found that the addition of 10% glycerol to hypotonic buffers greatly enhanced the yield of cell membrane fragments and improved TrkB immobilization. The TrkB receptors were immobilized on spherical magnetic iron oxide nanoclusters (a collection of individual iron oxide nanoparticles) to enable rapid isolation of binding compounds via magnetic separation. The iron oxide nanoclusters of about 200 nm were synthesized using a well-documented solvothermal method. 43,44 Here, the use of iron oxide nanoclusters had several advantages: (1) nanoclusters remain superparamagnetic but have much higher magnetic moments than individual superparamagnetic nanoparticles, which enables rapid magnetic separation; (2) the size is large enough to immobilize sufficient TrkB receptors on the surfaces but still small enough to remain as a colloidal suspension. Large iron oxide nanoparticles (>400 nm) precipitate out of the aqueous solution quickly. The solvothermal method involved first mixing reactants (iron chloride, sodium acetate, and polyacrylic acid) in ethylene glycol, a reducing solvent, under stirring; then, the mixture was reacted in a sealed Teflon-lined stainless steel hydrothermal reactor at 200 °C to induce iron oxide nanocluster formation.⁴⁵ Subsequently, the cell fragments and nanoclusters were incubated on ice for 30 min to induce CMMN formation followed by ultrasonication (27% amplitude) for 1 min and 20 s (5 s pulse on, 5 s pulse off) to create CMMNs.

Figure 2A shows a typical transmission electron microscopy (TEM) image of CMMNs created using cell membrane fragments from SH-SY5Y neuroblastoma cells overexpressing

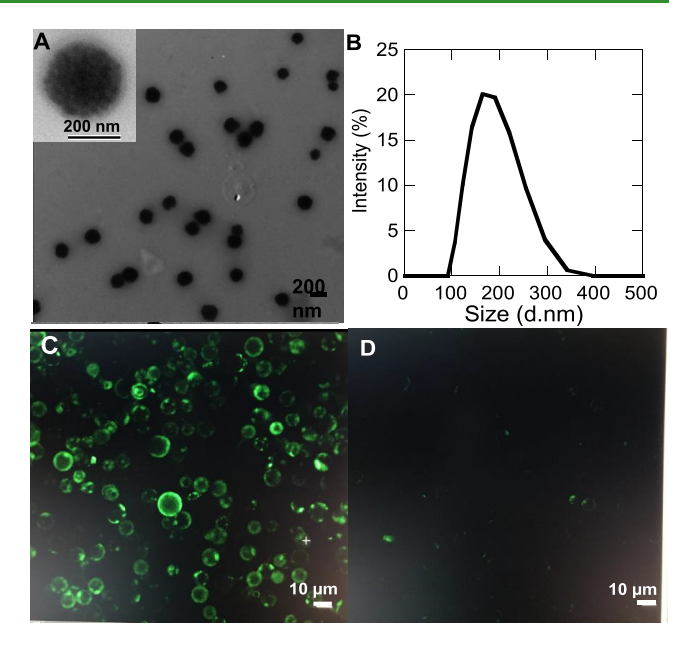


Figure 2. (A) TEM image of CMMNs with a closer view of a CMMN (inset), (B) DLS plot of CMMNs in bis—tris buffer, and confocal images of cell membrane fragments from cells overexpressing TrkB (C) and TrkB-null cells (D) immobilized on silica microbeads. The TrkB receptors were first incubated with BDNF and then labeled with the anti-BDNF primary antibody and fluorescence-labeled secondary antibody.

TrkB. Membrane coverage on the iron oxide nanocluster surfaces was clearly visible, indicated by the lighter shell (Figure 2A-inset). In contrast, iron oxide nanoclusters prior to cell membrane coating did not show any light shells (Figure S1). For CMMN formation, two parameters are essential: one is TrkB activity that determines the latter binder identification process through the specific interactions between receptors and binders; the other is the full encapsulation of the nanoclusters inside the cell membrane to eliminate nonspecific direct binding to nanocluster surfaces. Because a TEM image only represented a small number of CMMNs, the size and size distribution of CMMNs were also measured in a buffer solution using dynamic light scattering (DLS). The DLS plot showed an average size of CMMNs around 200 nm, similar to the size observed from the TEM image, indicating CMMNs in solution were free of aggregation or other sized free vesicles (Figure 2B).

In order to confirm the presence of TrkB on CMMN surfaces, CMMNs were incubated with BDNF and then labeled with the anti-BNDF primary antibody followed by detection with the fluorescence-labeled anti-IgG secondary antibody. Unfortunately, because of the size detection limit of confocal microscopy, these antibody-labeled CMMNs were not visible. Alternatively, cell membrane fragments prepared using SH-SY5Y neuroblastoma cells overexpressing TrkB were immobilized on silica microbeads. The cell membrane-covered microbeads were first incubated with BDNF and then labeled with the BDNF targeting primary antibody and fluorescencelabeled secondary antibody (Figure 2C). The intensive green shell indicated not only the high density of TrkB within the cell membrane fragments from SH-SY5Y neuroblastoma cells but also their interactions with BDNF. Here, cell membrane fragments obtained from a TrkB-null parental cell line were used as a negative control, which did not show much

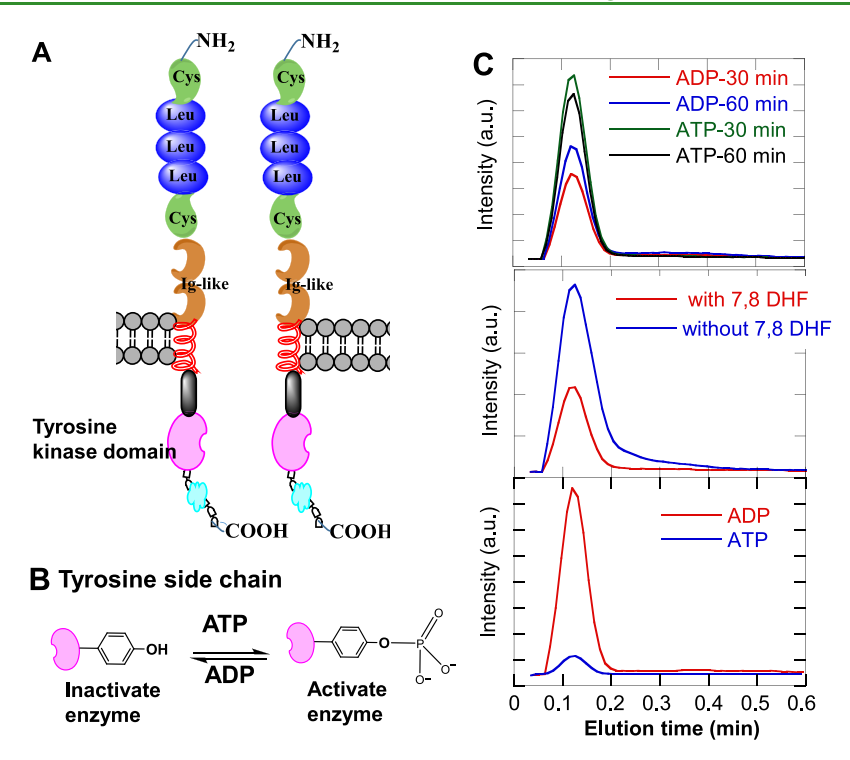


Figure 3. (A) Schematic representation of the TrkB structure, (B) tyrosine kinase activity-related reaction, an ATP dependent process, and (C) ESI-MS plots (negative ionization mode; ATP m/z 505.8; ADP m/z 425.9): (top) Levels of ATP and ADP after 30 and 60 min of incubation of CMMNs with 5 mM ATP and 100 μ M 7,8-DHF at 37 °C, (middle) levels of ATP after 30 min of incubation of CMMNs with 5 mM ATP and 100 μ M 7,8-DHF at at 37 °C, and (bottom) levels of ATP after 24 h of incubation of CMMNs with 5 mM ATP and 100 μ M 7,8-DHF at 4 °C.

detectable fluorescence (Figure 2D). The experiment performed in the presence of anti-BDNF antibody but without BDNF also resulted in the lack of fluorescence on the surface of silica beads. Silica beads prepared with TrkB-null cells and incubated with BDNF and anti-BDNF antibodies also showed no detectable fluorescence. For each step of labeling, silica beads were separated out of the solution by centrifugation and washed using ammonium acetate buffer (10 mM, pH 7.4, 0.5 mL) with 1% sodium cholate to remove any nonspecific binding.

Activity of the Immobilized TrkB on CMMNs. The activity of the immobilized TrkB is crucial for specific identification of binding compounds. TrkB has several distinct structural components, as shown in the schematic representation (Figure 3A). TrkB receptors exist in a dimer form, and the extracellular domains include three leucine-rich repeats surrounded by two cysteine-rich domains and immunoglobulin (Ig)-like domains close to the transmembrane regions. The Iglike domains are mainly responsible for TrkB agonist binding, and TrkB ligand binding causes TrkB dimerization and subsequent activation of the tyrosine kinase intracellular domain. Therefore, it is important to evaluate the TrkB activity related to tyrosine kinase. Figure 3B shows the typical reaction of tyrosine kinase in the presence of ATP. Here, we tested the activity of the immobilized TrkB receptors by monitoring the conversion of ATP to ADP, a process commonly performed by all types of tyrosine kinase receptors. Specifically, CMMNs with TrkB receptors were incubated with 5 mM ATP and 100 μ M of known activator 7,8-DHF at 37 °C for 30 or 60 min. The conversion was analyzed by electrospray ionization mass spectrometry (ESI-MS). The analysis was performed using direct injection of the analysis mixture onto

the mass spectrometer without prior separation on an analytical column; thus, the elution times were very short. Both ATP and ADP were monitored in the negative ionization mode. The conversion of ATP to ADP was clearly observed (Figure 3C-top) by the intensity change of the peaks. The TrkB activation by an activator is critical for the phosphorylation of kinase to convert ATP. CMMNs incubated with 5 mM ATP but without 7,8-DHF showed no significant reduction in the conversion of ATP to ADP (Figure 3Cmiddle). Similar ATP to ADP conversion was also observed with 5 mM ATP and 10 μ g/mL of BDNF at 37 °C for 30 min (Figure S2). To minimize the autoconversion of ATP to ADP at 37 °C, the same experiment was performed at 4 °C with 24 h of incubation, as shown in Figure 3C-bottom, where the ATP to ADP conversion was very pronounced. We also tested the possible involvement of nanoclusters (structures inside CMMNs) in the ATP-converting activity of TrkB receptors. The nanoparticles themselves did not lead to detectable ATP to ADP conversion when incubated with 5 mM ATP and 100 μ M 7,8-DHF at 37 °C. CMMNs prepared using the TrkB-null parental cell line were used as a negative control in the experiment. No ATP/ADP conversion was observed for nanoclusters encapsulated with TrkB-null cell membrane fragments. These ATP/ADP conversion studies suggested that the immobilized TrkB receptors remained active. We also attempted to measure phosphorylation of tyrosine residues using specific antibody targeting phosphorylated tyrosine. Unfortunately, we did not observe the phosphorylation, likely because the intracellular part of TrkB was directly interfaced with iron oxide nanoclusters. These nanointerfaces may hinder the access of the labeling antibody, which is more accessible in cells.

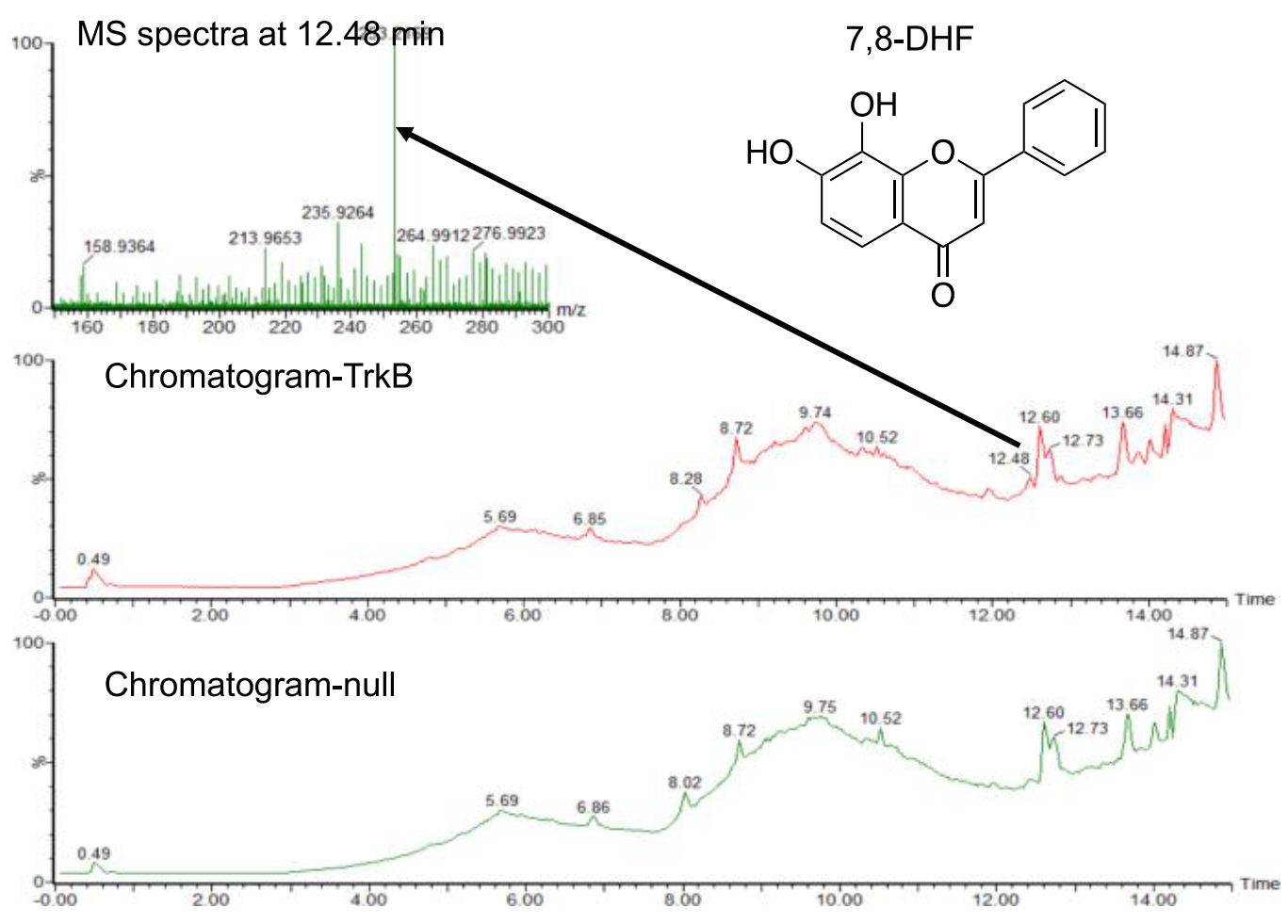


Figure 4. UPLC chromatogram of the elution profile from CMMNs from TrkB expressing and TrkB-null cells and QTof-MS spectrum of 7,8-DHF identified from an artificial mixture.

Direct quantification of the exact amount of TrkB on CMMNs is very challenging; therefore, the TrkB amount was estimated using two different methods. First, the protein concentrations of the cell membrane fragments from the same amount of parental TrkB-null control cells and TrkB overexpressing cells were quantified using a Bradford protein assay (Table S1). The difference in protein amounts between fragments from TrkB overexpressing cells, SH-SY5Y cells, and the parental TrkB-null cells was attributed to TrkB. After divided by the TrkB molecular weight, the total number of TrkB in the cell membrane fragment was obtained. With the experimentally determined CMMN concentration in each experiment, the number of TrkB per CMMN was roughly estimated to be in the range of 10^7-10^8 . This experiment assumed no cell membrane loss during the CMMN formation. Additionally, 250 μ L of CMMNs ($10^7/m$ L) was incubated with 250 μ L of 7,8-DHF buffer solution (1 μ M). After quantifying the amount of 7,8-DHF in the original solution and supernatant using the HPLC elution peak areas of 7,8-DHF, the difference subtracting the amounts of 7,8-DHF in the three washes was attributed to TrkB binding (Figure S3). Here, we assumed one-to-one TrkB and 7,8-DHF biding. The amount of TrkB per CMMN was then estimated to be in the range of 10⁶–10⁷ by using the amount of binding TrkB divided by the amount of CMMN⁷. The lower number of TrkB based on the fishing experiments suggested a loss of cell membrane fragments during the CMMN formation. Though those

estimations were rough, it provides some guidance on the ligand fishing experiment.

Screening with CMMNs. After TrkB activity confirmation, CMMNs with TrkB receptors were applied to screen compound mixtures with three different levels of complexity, including mixtures with known small molecule binders, synthetic small molecule mixtures containing 71 pure compounds, and Gotu Kola plant extracts. In biological systems, BDNF is the physiological agonist. However, as discussed earlier, BDNF cannot be used as a treatment option for neurological discorders. 12 Therefore, alternative molecules have been explored to stimulate TrkB receptors, 14,17-68 such as 7,8-DHF. 13,14,47,48 Thus, 7,8-DHF was used as a known binder to create an artificial mixture for initial screening. The artificial mixture consisted of equimolar concentrations (100 nM) of 7,8-DHF and non-binders: caffeic acid and rutin. Specifically, CMMNs ($\sim 10^7$) were incubated with 0.5 mL of the artificial mixture for 20 min at 37 °C. The CMMNs were then magnetically separated out of the mixture and washed three times with ammonium acetate buffer (10 mM, pH 7.4, 0.5 mL). After washing, the binders on CMMNs were eluted with 0.5 mL of buffer/methanol (9:1, v/v) mixture. In both washing and elution steps, the CMMNs were separated from the supernatant using a magnet. The elution profiles were analyzed by a quadrupole time-of-flight mass spectrometer (QTof-MS) with an ultrahigh-performance liquid chromatography (UPLC) system (Water Xevo G2xs QTof-MS with iclass UPLC). Figure

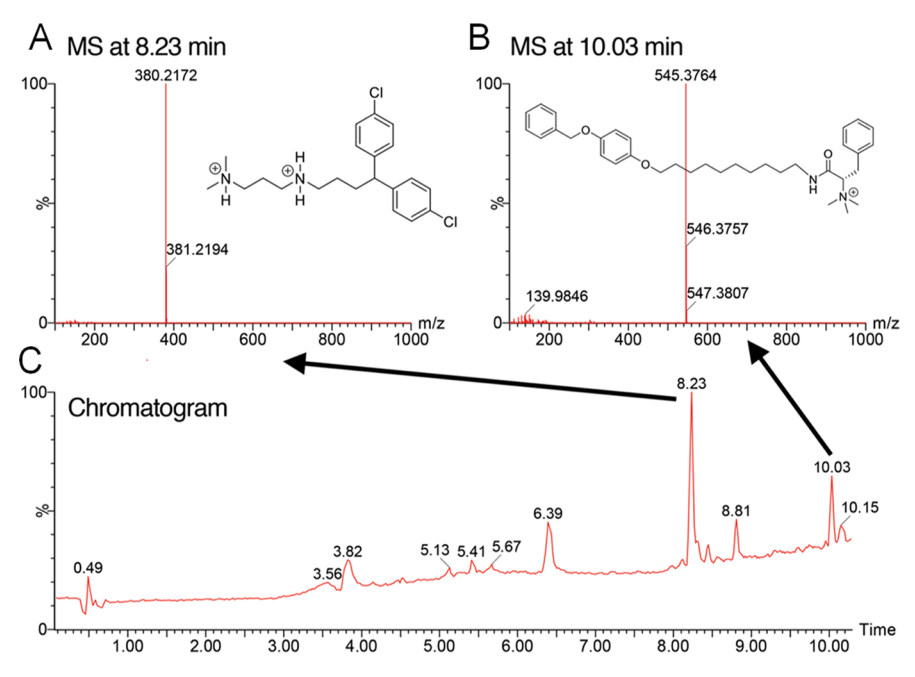


Figure 5. (A, B) QTof-MS spectra of two sample compounds identified using CMMNs and (c) UPLC chromatogram of the elution profile.

4 shows the UPLC chromatogram and QTof-MS spectrum of the eluted compound in negative ionization mode. The identity of all the analyzed compounds was confirmed by comparing retention times and m/z ratios with data obtained for the available standards. The CMMNs were able to selectively retain the known binder compared to the control, 7,8-DHF, which was released during the elution step close to 12.48 min confirmed by the mass spectrum. The CMMNs prepared with the parental SH-SY5Y cell line without TrkB showed no detectable binders. These results suggested that the immobilized TrkB receptors on CMMNs were able to fish out binding compounds. In contrast, the nonbinders were not detected in the elution profiles.

Subsequently, fishing experiments of CMMNs were conducted using a library containing 71 synthetic small molecules with equal molar concentration (1 μ M). The library was created by the in silico screening of a larger compound library (~1600 molecules) against the flecainide (a known ion channel blocker) binding site of the available cardiac Nav1.5 CryoEM structure⁴⁹ using SeeSAR (BioSolveIT). To perform the fishing experiment, CMMNs ($\sim 10^7$) were incubated with 0.5 mL of the library mixture for 20 min at 37 °C. After magnetic separation and three washes with ammonium acetate buffer (10 mM, pH 7.4, 0.5 mL), the CMMN-bound compounds were eluted with a buffer/methanol (1:9, v/v) mixture (0.5 mL). The elution profiles were analyzed by a Water Xevo G2xs QTof-MS with an iclass UPLC system. Figure 5 shows the UPLC chromatogram and QTof-MS spectra of two examples out of six total identified compounds. The compound SD-IV-252b eluted at 8.23 min with m/z of 380.2172 while the compound SV-VI-845-8 eluted at 10.03 min with m/z of 545.3764. Even though the library was not originally designed for TrkB, the fishing experiment clearly demonstrated the feasibility of the new CMMN platform to identify compounds interacting with TrkB from synthetic small molecule libraries.

Natural products have been shown to be an invaluable source of novel drugs.⁵⁰ For example, numerous compounds produced by plants have been developed into widely used

medicines, such as artemisinin and ivermectin. 51 In 2015, the Nobel Prize in Physiology or Medicine was awarded for the discovery of artemisinin isolated from Artemisia annua, a medicinal plant.⁵² The promising preclinical data of Gotu Kola extracts have convinced the FDA to approve the use of this extract for a clinical trial in patients with mild cognitive impairment.⁵³ The Gotu Kola plant extract has been shown to contain active metabolites for a wide range of pharmaceutical activities. 54,55 In particular, studies have shown the benefits of Gotu Kola in enhancing memory and neuroprotective activities. 56,57 However, the exact mechanism of action is not fully understood. Additionally, Gotu Kola extracts were shown to contain molecules that may potentially bind to TrkB, as they belong to the same group of phytochemicals as 7,8dihydroxyflavone, a compound that was previously described to activate TrkB receptors. The Gotu Kola extract is also the only currently FDA-approved extract to be tested in clinical trials for the prevention and/or treatment of AD. Therefore, Gotu Kola plant extracts were chosen to evaluate the drugscreening platform for the identification of TrkB binders.

The plant extracts were prepared by sonicating 200 mg of ground plant material in methanol (100%), methanol/water (50/50), and water for 20 min at room temperature. Following the extraction, 1 mL of the extract was aliquoted and the solvent was removed under a stream of nitrogen. The residue was resuspended in 1 mL of ammonium acetate buffer (10 mM, pH 7.4) and undissolved materials were removed by centrifugation (5000 rpm, 5 min). 0.5 mL of those extracts were subsequently used in the fishing experiments. In brief, CMMNs (\sim 10⁷) were incubated with 0.5 mL of Gotu Kola plant extracts for 20 min at 37 °C. After magnetic separation and three washes with 0.5 mL of ammonium acetate buffer, the binders on CMMNs were eluted with buffer/methanol mixtures (9/1-E1 5/5-E2 and 1/9-E3, v/v, 0.5 mL) and analyzed by a Water Xevo G2xs QTof-MS with an iclass UPLC. Most compounds were detected from elution 3 (E3) or elution 2 (E2). 100 and 50% methanol plant extracts showed similar compounds but with different relative amounts.

To exclude nonspecific binding, CMMNs were also prepared using parental TrkB-null cells as negative control for all the fishing experiments. Compounds that bind to CMMNs with functional TrkB but not bind to those control CMMNs from TrkB-null cells were marked as binders. Those binders were identified based on their elution time in ultrahigh-performance liquid chromatography (UPLC), and the corresponding compound masses were then obtained from QTof-MS. Figures S4-S7 show the analysis of UPLC chromatograms of three elutions for each plant extract screened by CMMNs prepared with both cell lines. Compounds that were observed in both types of CMMNs were marked as nonspecific binders, which were not analyzed here. The eluted compounds were analyzed in both negative and positive ionization mode using mass spectrometry. All of the compounds detected in the negative ion mode were observed in positive mode, but only some compounds detected in positive mode were shown in negative mode. Therefore, data from positive ionization mode were used to analyze the compound.

Figure 6 shows UPLC chromatograms and QTof-MS spectra of the identified compounds analyzed in positive

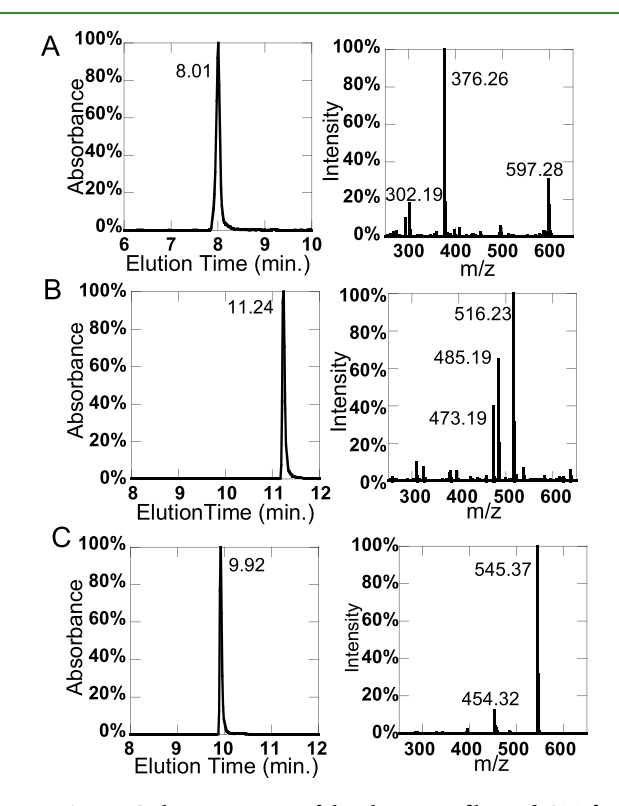


Figure 6. UPLC chromatograms of the elution profiles and QTof-MS spectra of compounds identified using CMMN from Gotu Kola plant extracts: (A) caffeoylquinic acids; (B) dicaffeoylquinic acids, pomolic acid or isomers, castillicetin; and (C) madecassic acid or its isomers and stigmasterol.

ionization mode. By comparing with a previous report with a complete list of bioactive compounds in Gotu Kola, ⁵⁶ these compounds can be tentatively identified as isomers of caffeoylquinic acids (MW 354.31) from E3 of 50% methanol extraction, which was detected at elution time 8.01 min with m/z of 376.26 ([M–H + Na]+), as shown in Figure 6A. Other detected masses in this elution included a detected m/z at 302.19 (possibly quercetin, MW 302.24) and a detected m/z at

597.28 (possibly naringin with a mass 580.54), and the detected m/z is the ion adducts of $[M-H + NH_4]^+$. Figure 6B shows the UPLC chromatogram at 11.2 min and the QTof-MS spectrum of the E3 elution from 100% methanol extraction, where the detected m/z 516.23 can be assigned as one of the isomers of dicaffeoylqunic acids (MW 516.4). In this elution, the detected m/z at 473.19 matched well with pomolic acid or its isomers (MW 472.7) and the detected m/z at 485.19 has a good match with castillicetin (MW 464.4). Figure 6C shows the UPLC chromatogram at 9.92 min and the QTof-MS spectrum of the E3 elution from 100% methanol extraction, where the detected m/z 545.37 can be assigned to madecassic acid or its isomers (MW 504.7), where the detected m/z is the ion adducts with acetonitrile (ACN) in the running phase of UPLC. The other detected m/z at 454.32 was the ACN adduct ion of stigmasterol.

Table 1 shows all of the identified possible compounds with their chemical structures, exact masses, and detected mass with the adduct ion index. Some of the compounds, such as dicaffeoylqunic acids and pomolic acid, have multiple isomers, but only one representative chemical structure is shown in Table 1. That detected mass was possible to be other types of isomers as well. Therefore, our future studies will include a comparison of different isomers, such as fishing experiments with CMMNs and TrkB activation.

In order to verify whether TrkB binding compounds were completely released during the elution processes, we also examined each eluted compound by quantifying the peak areas of the eluted compounds in UPLC chromatograms. The difference in peak areas of a compound between a plant extract before and after fishing was assigned to CMMN binding, which theoretically should match the sum of areas under the peaks of all washes and elutions for that particular compound. By comparing the peak area difference of a compound before and after fishing and the sum of the peak areas (washes and elutions), the amounts of binders retained on CMMNs were obtained. These comparisons in Figure S8 suggested that not all binding compounds were eluted. Depending on the compound, 30-50% of compounds were retained on CMMNs. For example, about 30% of the naringin was retained on CMMNs after washing and elution and the majority of the compound was eluted in elution 2 with 50/50 buffer/methanol. Our future studies will include optimization of elution solutions and correlate the elution with binding affinities.

Some of those identified compounds have been previously reported to have various neural related activities. For example, madecassic acid was reported to promote neurite elongation in hippocampal CA1 neurons. 58,59 Dicaffeoylquinic acid was shown to alleviate memory loss in depressed mice 60 and exhibited protective activity against β -amyloid toxicity. 61 The therapeutic potential of naringin was demonstrated in several neurological disorders, 62 including AD and PD. The neuroprotective role of quercetin was also well documented. 63,64 To evaluate whether the identified compounds are really activating TrkB, we tested the effects of one of the TrkB binding compound from Gotu Kola, 4-O-cafeoylquinic acid (4-O-COA) on dendritic arborization. Dendritic arborization is a functionally relevant in vitro endpoint as it reflects potential to modulate synaptic plasticity. TrkB has been reported to regulate neurite outgrowth, and dendritic complexity⁶⁵ and TrkB agonists have been shown to enhance dendritic arborization.66 Our preliminary experiments showed that

Table 1. Summary of the Identified Compounds from Gotu Kola Plant Extracts

Possible Compounds	Example Structures	Exact Mass (mw)	Detected Mass/Index
Dicaffeoylquinic acid	10 for form	516.46	516.12 [M+H] ⁺
O-Caffeoylquinic Acid	HO COSH	354.31	376.26 [M+Na-H]⁺
Madecassic acid	MO CH CH	504.7	545.37 [M+ACN+H]+
Castillicetin	HO OH OH	464.4	485.19 [M+Na-2H] ⁺
Quercetin	HO OH OH	302.24	302.19 M+
Stigmasterol	HO H	412.69	454.32 [M+ACN+H] ⁺
Pomolic acid	HO H OH	472.7	473.19 [M+H]*
Naringin	HO DH OH O	580.54	597.28 [M+H ₂ O-H] ⁺

treatment with 1 μ M 4-O-CQA increased the amount of dendritic complexity in isolated 5×FAD hippocampal neurons *in vitro* (Figure S9A). One week of treatment with the compound significantly increased arborization in these A β -expressing neurons *in vitro* (Figure S9B).

These fishing experiments suggested two important messages. First, the immobilized TrkB receptors on CMMNs can be used for rapid compound screening and TrkB can serve as a valid target. Second, the reported drug-screening platform is useful to evaluate the cellular pathways involved in the compound activity. As indicated by the Gotu Kola fishing experiments, phytochemicals in Gotu Kola with reported neuroprotective activities likely involve BDNF/TrkB pathway. Even though the screening experiments were only performed for one plant species, the feasibility and potential of TrkB as a target to screen natural product mixtures has been demonstrated, which can be easily applied to screen other natural mixtures.

CONCLUSIONS

In summary, functional TrkB receptors were successfully immobilized on magnetic iron oxide nanoclusters for compound identification. The presence of TrkB was confirmed with confocal microscopy *via* antibody labeling, and their activities on the nanocluster surfaces were verified by ATP/ADP conversion in the presence of a known TrkB agonist. Importantly, the immobilized TrkB receptors on CMMN surfaces were able to not only fish out the known binders from an artificial mixture but also identify binding compounds from synthetic small molecule mixtures. Most importantly, the fishing experiments with Gotu Kola plant extracts were able to identify several compounds, which matched well with previously reported neuroprotective compounds. These studies demonstrated the feasibility of using CMMNs as a drug-

screening platform and TrkB as a valid drug target. Our studies showed that the possible therapeutic effects of the Gotu Kola plant extract in dementia treatment, at least partially, might be associated with compounds interacting with TrkB. The immobilized TrkB platform can have a substantial impact on the discovery of TrkB agonists for neurological disorders. Even though only one transmembrane receptor is proposed, this assay can be readily adjusted to any other transmembrane protein targets.

■ EXPERIMENTAL SECTION

Materials. The following chemicals and reagents were purchased from VWR: ferric chloride (ACROS, 98% purity), sodium acetate (99%), ethylene glycol, sodium polyacrylate solution (Sigma Aldrich, 45% water, MW = 1200), RPMI 1640 medium (Invitrogen), fetal bovine serum (FBS, Thermo Scientific), penicillin/streptomycin (Thermo Scientific), Tris—HCl, NaCl (>99%), MgCl₂ (\geq 98%), CaCl₂ (\geq 99%), KCl (>99%), ammonium acetate (>99%), benzamidine hydrochloride (>99%), and EDTA (\geq 98%). Phenylmethanesulfonylfluoride (PMSF, \geq 98.5%), geneticin (G418), and all other chemicals were purchased from Sigma-Aldrich unless otherwise stated (St. Louis, MO). Silica microparticles were obtained from Regis Technologies (Morton Grove, USA).

Cell Culture and Preparation of Cell Membrane Fragments. SH-SY5Y cells overexpressing TrkB (Kerafast, ECP007) and parental TrkB-null cells (Kerafast, EPC004) were cultured following the manufacturer's protocols (RPMI 1640 media supplemented with 10% fetal bovine serum- FBS, 1% antibiotics of Pen/Strep, and 0.3 mg/mL G418 at 37 °C with 5% CO₂). Cells were passaged every 2–3 days after cells reached 80% confluency. Low-concentration trypsin (0.25%) was used to detach the cells. To prepare membrane fragments, 1×10^7 cells were collected and resuspended in 20 mL of buffer (Tris–HCl, 50 mM, pH 7.4, containing 5 mM EDTA, 100 mM NaCl, 2 mM MgCl₂, 3 mM CaCl₂, 5 mM KCl, 3 mM benzamidine, 0.1 mM PMSF, 10% glycerol, and 1/100 protease inhibitor cocktail). The addition of 10% glycerol in the buffer is critical for cell membrane

stability. The suspension was homogenized using a glass Dounce homogenizer and then centrifuged for 5 min at 4 $^{\circ}$ C at 400 g. The resulting pellet was discarded, and the supernatant was subsequently centrifuged for 10 min at 4 $^{\circ}$ C at 10,000 g. Finally, the cell membrane fragments were collected by centrifugation (45 min at 4 $^{\circ}$ C at 100,000 g). Cell membrane fragments were subsequently suspended in 3.0 mL of bis—tris buffer (20 mM, pH 7.2) for CMMN preparation.

Synthesis and Characterization of Iron Oxide Nanoclusters. The iron oxide nanoclusters (~200 nm) were synthesized using our well-established protocols^{43,44} by heating the reactants (iron chloride, sodium acetate, and PAA) in ethylene glycol in a sealed Teflon-lined stainless steel hydrothermal reactor at 200 °C. In brief, FeCl₃ (0.8 mmol, 0.129 g) was dissolved in 30 mL of ethylene glycol followed by the addition of PAA water solution (8 mmol, 0.52 g) and sodium acetate (35 mmol, 2.87 g). The mixture was stirred for 3 h at room temperature to obtain a well-dispersed clear solution before transferring into a 100 mL hydrothermal reactor. After a 12 h reaction at 200 °C, the iron oxide nanoclusters were collected from the hydrothermal reactor and then washed three times with deionized water and ethanol in a 1:4 volume ratio. After drying under vacuum, the nanoclusters were weighed and re-dispersed in deionized water to prepare 1 mg/mL solution for CMMN formation.

Preparation of Cell Membrane-Encapsulated Magnetic Nanoclusters (CMMNs). CMMNs were prepared by first mixing 3 mL of cell membrane fragment solution from 10⁷ cells with 1.0 mL of sterilized 1.0 mg/mL PAA-coated nanoclusters. The mixture was vortexed briefly and incubated on ice for 30 min at room temperature. Then, the mixture was tip sonicated for 120 s (27% amplitude, 5 s on, 5 s off) using a Branson digital sonifier with a one-eighth inch microtip. CMMNs with TrkB were stored at 4 °C for further experiments.

Characterization of CMMNs. The size and morphology of the CMMNs were examined under TEM by simply dropping the CMMN buffer solution on a carbon-coated TEM copper grid using a Hitachi transmission electron microscope. The overall size and size distribution in solution was tested by dispersing 200 μ L of CMMN solution in 800 μ L of buffers using a Melvern Nanosizer instrument. To prepare samples for confocal imaging, the cell membrane fragments were immobilized on silica microbeads and imaged using a Nikon C2 confocal microscope.

Confocal Microscopy Analysis. The presence of TrkB receptors on the cell membrane fragments was studied by immobilizing cell membrane fragments onto silica microbeads followed by antibody labeling and confocal microscopy imaging. In brief, freshly prepared cell membrane fragments from TrkB and TrkB-null cells (10⁻⁷) were prepared and suspended in 1 mL of ammonium acetate buffer containing 1 mg of silica beads. 100 μ L of this mixture was incubated with 400 μ L of BDNF (final concentration of 100 μ M) for 1 h at room temperature. The cell membrane-coated beads were separated out of solution by centrifugation (1 min, 10,000 g) and washed three times with ammonium acetate buffer. The pellet was then incubated with 1% goat serum and the anti-rabbit BDNF primary antibody (1:50) in 250 µL of ammonium acetate buffer at 4 °C overnight with rocking. After removing excess antibodies with centrifugation (1 min, 10,000 g), the pellet was washed three times with 0.5 mL of ammonium acetate buffer containing 1% sodium cholate. Finally, the pellet was incubated with 1% goat serum and the secondary antibody with fluorophore (1:1000) overnight at 4 °C. After removing excess secondary antibodies and washing, the pellet was resuspendeded in 50 μL of ammonium acetate buffer, and 20 μL was loaded on the slide. The plated samples were imaged with a Nikon C2 laser scanning camera using a GFP filter.

TrkB Activity. The TrkB activity was studied by monitoring ATP to ADP conversion due to tyrosine phosphorylation upon TrkB activation, a process commonly performed by functional TrkB. Briefly, 0.5 mL of CMMN solution (50 mM ammonium acetate buffer, pH 7.4) was incubated with 5 mM ATP and 100 μ M TrkB activator (7–8 DHF) at 37 °C for 30 or 60 min. The negative control experiment was performed without 100 μ M TrkB activator (7–8 DHF). To reduce autoconversion of ATP to ADP at 37 °C, the same experiment

was also performed at 4 $^{\circ}$ C overnight. After incubation, the CMMNs were magnetically separated, and the supernatants were analyzed by ESI-MS. The analysis was performed using direct injection of analytes into the mass spectrometer without prior separation on an analytical column, hence very short elution times. Both ATP and ADP were monitored in negative ionization mode (ATP m/z 505.8; ADP m/z 425.9).

Estimation of TrkB Amounts. The amount of TrkB on each CMMN was estimated using two different methods. First, the protein concentrations of the cell membrane fragments from the same amount of parental TrkB-null control cells and TrkB overexpressing cells were quantified using the Bradford protein assay (Table S1). The difference in protein amounts between fragments from TrkB overexpressing cells, SH-SY5Y cells, and the parental TrkB-null cells was attributed to TrkB. After divided by the molecular weight of TrkB, the total number of TrkB was obtained. With the experimentally determined CMMN concentration in each experiment, the number of TrkB per CMMN was roughly estimated. Additionally, 250 μ L of CMMNs (10⁷/mL) was incubated with 250 μ L of 7,8-DHF buffer solution (1 μ M) at 37 °C for 20 min. After magnetic separation and three washes with ammonium acetate buffer (10 mM, pH 7.4, 0.25 mL), 7,8-DHF was eluted using a mixture of ammonium acetate/ methanol (9/1, 1/1, 1/9 v/v; 0.25 mL). The elution profiles were analyzed by an HPLC-MS system. After quantifying the amount of 7,8-DHF in the original solution and supernatant using the HPLC elution peak areas of 7,8-DHF, the difference subtracting 7,8-DHF in washing buffers was attributed to TrkB binding and the amount of TrkB per CMMN was then estimated.

Fishing Experiments. The fishing experiments were performed using three screening sources: an artificial mixture containing an equal molar amount (100 nM) of known TrkB binder (7-8 DHF) and nonbinders (caffeic acid and rutin), a library of 71 synthetic molecules (1 µM of each compound), and Gotu Kola plant extract. For each fishing experiment, CMMNs ($\sim 10^7$) were incubated with 0.5 mL of an artificial mixture, synthetic library, or plant extracts for 20 min at 37 °C. After magnetic separation and three washes with ammonium acetate buffer (10 mM, pH 7.4, 0.5 mL), the binders on CMMNs were eluted with a mixture of buffer/methanol (1/9, 5/5 or 1/9 v/v, 0.5 mL). The elution profiles were analyzed by a Water Xevo G2xsQTof-MS with an iclass UPLC system. In order to verify whether the TrkB binding compounds were completely released during the elution processes, we also quantified the eluted compounds by comparing the difference in peak areas (due to binding) of plant extracts before and after fishing and the sum of peak areas of all washes and elutions for a particular compound. The comparisons suggested that not all binding compounds were eluted. Depending on the compounds, 30-50% of the compounds were retained on CMMNs. Our future studies will include seeking more effective elution solutions and correlate the elution with binding affinities. The comparison for each compound is shown in Figures S4-S7.

Dendritic Arborization in Isolated A β -Overexpressing Hippocampal Neurons. Primary neurons were generated from the 5×FAD mouse model of β -amyloid (A β) accumulation. These mice came from a founder breeding pair from The Jackson Laboratory (cat# 006554). The background strain for these mice and the strain of the non-transgenic wild-type littermates is B6SJLF1/J. Embryos from these mice were harvested to generate primary neurons. Hippocampal neurons were isolated as described in Kaech and Banker. 67 Briefly embryos were harvested at embryonic day 18. Hippocampi were subdissected from embryos, gently minced, and trypsinized to generate suspensions of dispersed neurons. These neurons were plated on poly-L-lysine-coated glass coverslips at a density of 130,000 cells per 60 mm dish containing 4 coverslips in MEM medium (Life Technologies), 5% FBS (Atlanta Biologicals), and 0.6% glucose (Sigma-Aldrich). After 4 h, coverslips were flipped cell side down into 60 mm dishes containing neural stem cell-derived glial cells and maintained in Neurobasal Medium supplemented with 1× GlutaMAX (Life Technologies) and 1× B-27Plus (Life Technologies). Dishes were fed every week by removing 1 mL of the culture medium and adding 1 mL of fresh Neurobasal Media containing GlutaMAX and B-

27 Plus, with the first feed (at 5 days *in vitro*) containing 6 μ M cytosine β -D-arabinofuranoside hydrochloride (AraC; Sigma-Aldrich). At 12 days *in vitro*, the cell culture feeding contained either 4-O-CQA (1 μ M) or DMSO. At 19 days, coverslips were fixed in 4% paraformaldehyde, rinsed in PBST, and stained with anti-MAP2B (Sigma-Aldrich #M4403; 3.3 μ g/mL) and goat anti-mouse IgG1-Cy3 (Jackson ImmunoResearch #115–165-205; 1.5 μ g/mL). Stained neurons were imaged using a Zeiss ApoTome2 microscope, blinded, and analyzed for morphology via the Sholl method by using Fiji software. ⁶⁸ We measured 30 non-overlapping, easily isolatable neurons per coverslip, and four coverslips per condition.

ASSOCIATED CONTENT

5 Supporting Information

The Supporting Information is available free of charge at https://pubs.acs.org/doi/10.1021/acsabm.1c00552.

TEM images of iron oxide nanoclusters and CMMNs from different bathes; ATP-to-ADP conversion experiments by BDNF; TrkB number estimation using the Bradford assay and ligand binding; binder identification from Gotu Kola extracts based on UPLC chromatograms and MS spectra; binder retention analysis on CMMNs after elution based on UPLC chromatograms; dendritic arborization test using 4-O-CQA (PDF)

AUTHOR INFORMATION

Corresponding Authors

Lukasz M. Ciesla — Department of Biological Sciences, The University of Alabama, Tuscaloosa, Alabama 35487, United States; orcid.org/0000-0003-2766-3667; Phone: 205-348-1828; Email: lmciesla@ua.edu

Yuping Bao — Chemical and Biological Engineering, The University of Alabama, Tuscaloosa, Alabama 35487, United States; orcid.org/0000-0003-2829-4082; Phone: 205-348-9869; Email: ybao@eng.ua.edu

Authors

Zekiye Ceren Arituluk – Department of Biological Sciences, The University of Alabama, Tuscaloosa, Alabama 35487, United States; Department of Pharmaceutical Botany, Hacettepe University, Ankara 06100, Turkey

Jesse Horne — Chemical and Biological Engineering, The University of Alabama, Tuscaloosa, Alabama 35487, United States; Present Address: Department of Chemical and Biomolecular Engineering, The University of Illinois at Urbana-Champaign, 114 Roger Adams Laboratory, MC 712 600 South Mathews Avenue, Urbana, Illinois 61801, United States

Bishnu Adhikari — Department of Biological Sciences, The University of Alabama, Tuscaloosa, Alabama 35487, United States

Jeffrey Steltzner — Department of Biological Sciences, The University of Alabama, Tuscaloosa, Alabama 35487, United States

Shomit Mansur — Chemical and Biological Engineering, The University of Alabama, Tuscaloosa, Alabama 35487, United States

Parmanand Ahirwar – Department of Chemistry, University of Alabama at Birmingham, Birmingham, Alabama 35294, United States

Sadanandan E. Velu — Department of Chemistry, University of Alabama at Birmingham, Birmingham, Alabama 35294, United States; orcid.org/0000-0002-0342-2378

Nora E. Gray – Department of Neurology, Oregon Health and Science University, Portland, Oregon 97239, United States

Complete contact information is available at: https://pubs.acs.org/10.1021/acsabm.1c00552

Author Contributions

The manuscript was written through contributions of all authors. All authors have given approval to the final version of the manuscript.

Notes

The authors declare no competing financial interest. This work was supported by NSF-CBET 1915873 and Merrymac-McKinley Foundation Award.

ACKNOWLEDGMENTS

This work was supported by NSF-CBET 1915873 and Merrymac-McKcinley Foundation Award. Y. B. and L.M.C. acknowledge the Alabama Life Research Institute for seed funding support and the University of Alabama Department of Biological Sciences for the use of TEM and confocal microscopy.

ABBREVIATIONS

BDNF, brain-derived neurotrophic factor; TrkB, tyrosine receptor kinase B; CMMNs, cell-membrane encapsulated magnetic nanoclusters; PAA, polyacrylate; TEM, transmission electron microscopy; DLS, dynamic light scattering; UPLC, ultrahigh-performance liquid chromatography; MS, mass spectrometry

REFERENCES

- (1) Fernández-Ruiz, J. The biomedical challenge of neurodegenerative disorders: an opportunity for cannabinoid-based therapies to improve on the poor current therapeutic outcomes. *Br. J. Pharmacol.* **2019**, *176*, 1370–1383.
- (2) Salamon, A.; Zádori, D.; Szpisjak, L.; Klivényi, P.; Vécsei, L. Neuroprotection in Parkinson's disease: facts and hopes. *J. Neural Transm.* **2020**, 127, 821–829.
- (3) Cao, J.; Hou, J.; Ping, J.; Cai, D. Advances in developing novel therapeutic strategies for Alzheimer's disease. *Mol. Neurodegener.* **2018**, *13*, 64.
- (4) Harrison, J. R.; Owen, M. J. Alzheimer's disease: the amyloid hypothesis on trial. *Br. J. Psychiatry* **2016**, *208*, 1–3.
- (5) Ayaz, M.; Sadiq, A.; Junaid, M.; Ullah, F.; Ovais, M.; Ullah, I.; Ahmed, J.; Shahid, M. Flavonoids as Prospective Neuroprotectants and Their Therapeutic Propensity in Aging Associated Neurological Disorders. *Front. Aging Neurosci.* **2019**, *11*, 155.
- (6) Ferrer, I.; Marín, C.; Rey, M. J.; Ribalta, T.; Goutan, E.; Blanco, R.; Tolosa, E.; Martí, E. BDNF and full-length and truncated TrkB expression in Alzheimer disease. Implications in therapeutic strategies. *J. Neuropathol. Exp. Neurol.* **1999**, *58*, 729–739.
- (7) Numakawa, T.; Odaka, H.; Adachi, N. Actions of Brain-Derived Neurotrophin Factor in the Neurogenesis and Neuronal Function, and Its Involvement in the Pathophysiology of Brain Diseases. *Int. J. Mol. Sci.* **2018**, *19*, 3650.
- (8) Giacobbo, B. L.; Doorduin, J.; Klein, H. C.; Dierckx, R. A. J. O.; Bromberg, E.; de Vries, E. F. J. Brain-Derived Neurotrophic Factor in Brain Disorders: Focus on Neuroinflammation. *Mol. Neurobiol.* **2019**, *56*, 3295–3312.
- (9) Wang, Z.-H.; Xiang, J.; Liu, X.; Yu, S. P.; Manfredsson, F. P.; Sandoval, I. M.; Wu, S.; Wang, J.-Z.; Ye, K. Deficiency in BDNF/ TrkB Neurotrophic Activity Stimulates δ-Secretase by Upregulating C/EBP β in Alzheimer's Disease. *Cell Rep.* **2019**, 28, 655–669.e5.

- (10) Giuffrida, M. L.; Copani, A.; Rizzarelli, E. A promising connection between BDNF and Alzheimer's disease. *Aging* **2018**, *10*, 1791–1792.
- (11) Ando, S.; Kobayashi, S.; Waki, H.; Kon, K.; Fukui, F.; Tadenuma, T.; Iwamoto, M.; Takeda, Y.; Izumiyama, N.; Watanabe, K.; Nakamura, H. Animal model of dementia induced by entorhinal synaptic damage and partial restoration of cognitive deficits by BDNF and carnitine. *J. Neurosci. Res.* **2002**, *70*, 519–527.
- (12) Pilakka-Kanthikeel, S.; Atluri, V. S. R.; Sagar, V.; Saxena, S. K.; Nair, M. Targeted brain derived neurotropic factors (BDNF) delivery across the blood-brain barrier for neuro-protection using magnetic nano carriers: an in-vitro study. *PLoS One* **2013**, *8*, No. e62241.
- (13) Jang, S.-W.; Liu, X.; Yepes, M.; Shepherd, K. R.; Miller, G. W.; Liu, Y.; Wilson, W. D.; Xiao, G.; Blanchi, B.; Sun, Y. E.; Ye, K. A selective TrkB agonist with potent neurotrophic activities by 7,8-dihydroxyflavone. *Proc. Natl. Acad. Sci. U. S. A.* **2010**, *107*, 2687–2692.
- (14) Liu, C.; Chan, C. B.; Ye, K. 7,8-dihydroxyflavone, a small molecular TrkB agonist, is useful for treating various BDNF-implicated human disorders. *Transl. Neurodegener.* **2016**, *5*, 2.
- (15) Fischer, D. L.; Sortwell, C. E. BDNF provides many routes toward STN DBS-mediated disease modification. *Mov. Disord.* **2019**, 34, 22–34.
- (16) Zhang, Z.; Liu, X.; Schroeder, J. P.; Chan, C.-B.; Song, M.; Yu, S. P.; Weinshenker, D.; Ye, K. 7,8-dihydroxyflavone prevents synaptic loss and memory deficits in a mouse model of Alzheimer's disease. *Neuropsychopharmacology* **2014**, *39*, 638–650.
- (17) Massa, S. M.; Yang, T.; Xie, Y.; Shi, J.; Bilgen, M.; Joyce, J. N.; Nehama, D.; Rajadas, J.; Longo, F. M. Small molecule BDNF mimetics activate TrkB signaling and prevent neuronal degeneration in rodents. *J. Clin. Invest.* **2010**, *120*, 1774–1785.
- (18) Edelbrock, A. N.; Àlvarez, Z.; Simkin, D.; Fyrner, T.; Chin, S. M.; Sato, K.; Kiskinis, E.; Stupp, S. I. Supramolecular Nanostructure Activates TrkB Receptor Signaling of Neuronal Cells by Mimicking Brain-Derived Neurotrophic Factor. *Nano Lett.* **2018**, *18*, 6237–6247.
- (19) Chen, Y.; Wang, H.; Chen, Y.; Wang, M.; Ding, G.; Li, T. Trk inhibitor GNF-5837 suppresses the tumor growth, survival and migration of renal cell carcinoma. *Oncol. Rep.* **2019**, 42, 2039–2048.
- (20) Meng, L.; Liu, B.; Ji, R.; Jiang, X.; Yan, X.; Xin, Y. Targeting the BDNF/TrkB pathway for the treatment of tumors. *Oncol. Lett.* **2018**, 17, 2031–2039.
- (21) Lange, A. M.; Lo, H.-W. Inhibiting TRK Proteins in Clinical Cancer Therapy. *Cancers* **2018**, *10*, 105.
- (22) Thomaz, A.; Jaeger, M.; Buendia, M.; Bambini-Junior, V.; Gregianin, L. J.; Brunetto, A. L.; Brunetto, A. T.; de Farias, C. B.; Roesler, R. BDNF/TrkB Signaling as a Potential Novel Target in Pediatric Brain Tumors: Anticancer Activity of Selective TrkB Inhibition in Medulloblastoma Cells. *J. Mol. Neurosci.* **2016**, 59, 326–333.
- (23) Zhang, C.; Li, X.; Gao, D.; Ruan, H.; Lin, Z.; Li, X.; Liu, G.; Ma, Z.; Li, X. The prognostic value of over-expressed TrkB in solid tumors: a systematic review and meta-analysis. *Oncotarget* **2017**, *8*, 99394–99401.
- (24) Arita, M.; Koike, J.; Yoshikawa, N.; Kondo, M.; Hemmi, H. Licochalcone A Inhibits *BDNF* and *TrkB* Gene Expression and Hypoxic Growth of Human Tumor Cell Lines. *Int. J. Mol. Sci.* **2020**, 21, 506.
- (25) Bull, S. C.; Doig, A. J. Properties of Protein Drug Target Classes. *PLoS One* **2015**, *10*, No. e0117955.
- (26) Overington, J. P.; Al-Lazikani, B.; Hopkins, A. L. How many drug targets are there? *Nat. Rev. Drug Discovery* **2006**, *5*, 993–996.
- (27) Terstappen, G. C.; Reggiani, A. *In silico* research in drug discovery. *Trends Pharmacol. Sci.* **2001**, 22, 23–26.
- (28) Cieśla, Ł.; Moaddel, R. Comparison of analytical techniques for the identification of bioactive compounds from natural products. *Nat. Prod. Rep.* **2016**, 33, 1131–1145.
- (29) Ciesla, L.; Okine, M.; Rosenberg, A.; Dossou, K. S. S.; Toll, L.; Wainer, I. W.; Moaddel, R. Development and characterization of the $\alpha 3\beta 4\alpha 5$ nicotinic receptor cellular membrane affinity chromatography

- column and its application for on line screening of plant extracts. *J. Chromatogr. A* **2016**, *1431*, 138–144.
- (30) Merkouris, S.; Barde, Y.-A.; Binley, K. E.; Allen, N. D.; Stepanov, A. V.; Wu, N. C.; Grande, G.; Lin, C.-W.; Li, M.; Nan, X.; Chacon-Fernandez, P.; DiStefano, P. S.; Lindsay, R. M.; Lerner, R. A.; Xie, J. Fully human agonist antibodies to TrkB using autocrine cellbased selection from a combinatorial antibody library. *Proc. Natl. Acad. Sci. U. S. A.* **2018**, *115*, E7023–E7032.
- (31) Harvey, A. L.; Edrada-Ebel, R.; Quinn, R. J. The re-emergence of natural products for drug discovery in the genomics era. *Nat. Rev. Drug Discovery* **2015**, *14*, 111–129.
- (32) Atanasov, A. G.; Waltenberger, B.; Pferschy-Wenzig, E.-M.; Linder, T.; Wawrosch, C.; Uhrin, P.; Temml, V.; Wang, L.; Schwaiger, S.; Heiss, E. H.; Rollinger, J. M.; Schuster, D.; Breuss, J. M.; Bochkov, V.; Mihovilovic, M. D.; Kopp, B.; Bauer, R.; Dirsch, V. M.; Stuppner, H. Discovery and resupply of pharmacologically active plant-derived natural products: A review. *Biotechnol. Adv.* 2015, 33, 1582–1614.
- (33) González-Mariscal, I.; Krzysik-Walker, S. M.; Doyle, M. E.; Liu, Q.-R.; Cimbro, R.; Santa-Cruz Calvo, S.; Ghosh, S.; Cieśla, L.; Moaddel, R.; Carlson, O. D.; Witek, R. P.; O'Connell, J. F.; Egan, J. M. Human CB1 Receptor Isoforms, present in Hepatocytes and β -cells, are Involved in Regulating Metabolism. *Sci. Rep.* **2016**, *6*, 33302.
- (34) Moaddel, R.; Wainer, I. W. The preparation and development of cellular membrane affinity chromatography columns. *Nat. Protoc.* **2009**, *4*, 197–205.
- (35) Wubshet, S. G.; Brighente, I. M. C.; Moaddel, R.; Staerk, D. Magnetic Ligand Fishing as a Targeting Tool for HPLC-HRMS-SPE-NMR: α-Glucosidase Inhibitory Ligands and Alkylresorcinol Glycosides from Eugenia catharinae. J. Nat. Prod. 2015, 78, 2657–2665.
- (36) Stephen, C.; El Omri, A.; Ciesla, L. Cellular membrane affinity chromatography (CMAC) in drug discovery from complex natural matrices. *ADMET DMPK* **2018**, *6*, 200–214.
- (37) McFadden, M. J.; Junop, M. S.; Brennan, J. D. Magnetic "Fishing" Assay To Screen Small-Molecule Mixtures for Modulators of Protein—Protein Interactions. *Anal. Chem.* **2010**, *82*, 9850—9857.
- (38) Zhu, Y.-T.; Ren, X.-Y.; Yuan, L.; Liu, Y.-M.; Liang, J.; Liao, X. Fast identification of lipase inhibitors in oolong tea by using lipase functionalised Fe₃O₄ magnetic nanoparticles coupled with UPLC-MS/MS. Food Chem. **2015**, 173, 521–526.
- (39) Mani, V.; Wasalathanthri, D. P.; Joshi, A. A.; Kumar, C. V.; Rusling, J. F. Highly Efficient Binding of Paramagnetic Beads Bioconjugated with 100 000 or More Antibodies to Protein-Coated Surfaces. *Anal. Chem.* **2012**, *84*, 10485–10491.
- (40) Tang, C.; Liu, Z.-S.; Qin, N.; Xu, L.; Duan, H.-Q. Novel Cell Membrane Capillary Chromatography for Screening Active Compounds from Natural Products. *Chromatographia* **2013**, *76*, 697–701.
- (41) Ding, X.; Chen, X.; Cao, Y.; Jia, D.; Wang, D.; Zhu, Z.; Zhang, J.; Hong, Z.; Chai, Y. Quality improvements of cell membrane chromatographic column. *J. Chromatogr. A* **2014**, *1359*, 330–335.
- (42) Sherwood, J.; Sowell, J.; Beyer, N.; Irvin, J.; Stephen, C.; Antone, A. J.; Bao, Y.; Ciesla, L. M. Cell-membrane coated iron oxide nanoparticles for isolation and specific identification of drug leads from complex matrices. *Nanoscale* **2019**, *11*, 6352–6359.
- (43) Antone, A. J.; Sun, Z.; Bao, Y. Preparation and Application of Iron Oxide Nanoclusters. *Magnetochemistry* **2019**, *5*, 45.
- (44) Mansur, S.; Rai, A.; Holler, R. A.; Mewes, T.; Bao, Y. Synthesis and characterization of iron oxide superparticles with various polymers. *J. Magn. Magn. Mater.* **2020**, *515*, 167265.
- (45) Gao, J.; Ran, X.; Shi, C.; Cheng, H.; Cheng, T.; Su, Y. One-step solvothermal synthesis of highly water-soluble, negatively charged superparamagnetic Fe₃O₄ colloidal nanocrystal clusters. *Nanoscale* **2013**, *5*, 7026–7033.
- (46) Todd, D.; Gowers, I.; Dowler, S. J.; Wall, M. D.; McAllister, G.; Fischer, D. F.; Dijkstra, S.; Fratantoni, S. A.; van de Bospoort, R.; Veenman-Koepke, J.; Flynn, G.; Arjomand, J.; Dominguez, C.; Munoz-Sanjuan, I.; Wityak, J.; Bard, J. A. A Monoclonal Antibody TrkB Receptor Agonist as a Potential Therapeutic for Huntington's Disease. *PLoS One* **2014**, *9*, No. e87923.

- (47) Chen, L.; Gao, X.; Zhao, S.; Hu, W.; Chen, J. The Small-Molecule TrkB Agonist 7, 8-Dihydroxyflavone Decreases Hippocampal Newborn Neuron Death After Traumatic Brain Injury. J. Neuropathol. Exp. Neurol. 2015, 74, 557–567.
- (48) Liu, X.; Chan, C.-B.; Qi, Q.; Xiao, G.; Luo, H. R.; He, X.; Ye, K. Optimization of a Small Tropomyosin-Related Kinase B (TrkB) Agonist 7,8-Dihydroxyflavone Active in Mouse Models of Depression. *J. Med. Chem.* **2012**, *55*, 8524–8537.
- (49) Jiang, D.; Shi, H.; Tonggu, L.; Gamal El-Din, T. M.; Lenaeus, M. J.; Zhao, Y.; Yoshioka, C.; Zheng, N.; Catterall, W. A. Structure of the Cardiac Sodium Channel. *Cell* **2020**, *180*, 122–134.e10. e10.
- (50) Bioactive Compounds from Natural Sources: Natural Products as Lead Compounds in Drug Discovery. Second edition ed.; CRC Press: New York, 2011; p 648.
- (51) Shen, B. A New Golden Age of Natural Products Drug Discovery. Cell 2015, 163, 1297–1300.
- (52) Croft, S. L.; Ward, S. The Nobel Prize in Medicine 2015: Two drugs that changed global health. *Sci. Transl. Med.* 2015, 7, 316ed14.
- (53) Pharmacokinetics Centella Asiatica Product (CAP) in Mild Cognitive Impairment. https://clinicaltrials.gov/ct2/show/NCT03937908?term=gotu+kola&rank=3.
- (54) Gohil, K. J.; Patel, J. A.; Gajjar, A. K. Pharmacological Review on Centella asiatica: A Potential Herbal Cure-all. *Indian J. Pharm. Sci.* **2010**, *72*, 546–556.
- (55) Sharma, R.; Kuca, K.; Nepovimova, E.; Kabra, A.; Rao, M. M.; Prajapati, P. K. Traditional Ayurvedic and herbal remedies for Alzheimer's disease: from bench to bedside. *Expert Rev. Neurother.* **2019**, *19*, 359–374.
- (56) Gray, N. E.; Magana, A. A.; Lak, P.; Wright, K. M.; Quinn, J.; Stevens, J. F.; Maier, C. S.; Soumyanath, A. *Centella asiatica*: phytochemistry and mechanisms of neuroprotection and cognitive enhancement. *Phytochem. Rev.* **2018**, *17*, 161–194.
- (57) Rao, M. K.; Rao, M. S.; Rao, G. S. Treatment with Centalla asiatica (Linn) fresh leaf extract enhances learning ability and memory retention power in rats. *Neurosci. J.* **2007**, *12*, 236–241.
- (58) Siddiqui, S.; Khan, F.; Jamali, K. S.; Musharraf, S. G. Madecassic Acid Reduces Fast Transient Potassium Channels and Promotes Neurite Elongation in Hippocampal CA1 Neurons. CNS Neurol. Disord.: Drug Targets 2020, 19, 12–26.
- (59) Wang, P.; Long, T.-F.; Wang, L._. P.; Song, J. Synergistic Effect of Asiatic Acid and Madecassic Acid against Antioxidant Deficit in Rat Peripheral Nervous System. *Int. J. Pharmacol.* **2019**, *15*, 837–843.
- (60) Lim, D. W.; Park, J.; Jung, J.; Kim, S.-H.; Um, M. Y.; Yoon, M.; Kim, Y. T.; Han, D.; Lee, C.; Lee, J. Dicaffeoylquinic acids alleviate memory loss via reduction of oxidative stress in stress-hormone-induced depressive mice. *Pharmacol. Res.* **2020**, *161*, 105252.
- (61) Gray, N. E.; Morré, J.; Kelley, J.; Maier, C. S.; Stevens, J. F.; Quinn, J. F.; Soumyanath, A. Caffeoylquinic Acids in *Centella asiatica* Protect against Amyloid- β Toxicity. *J. Alzheimer's Dis.* **2014**, 40, 359–373.
- (62) Ahmed, S.; Khan, H.; Aschner, M.; Hasan, M. M.; Hassan, S. T. S. Therapeutic potential of naringin in neurological disorders. *Food Chem. Toxicol.* **2019**, *132*, 110646.
- (63) Rifaai, R. A.; Mokhemer, S. A.; Saber, E. A.; Abd El-Aleem, S. A.; El-Tahawy, N. F. G. Neuroprotective effect of quercetin nanoparticles: A possible prophylactic and therapeutic role in alzheimer's disease. *J. Chem. Neuroanat.* **2020**, *107*, 101795.
- (64) Amanzadeh, E.; Esmaeili, A.; Rahgozar, S.; Nourbakhshnia, M. Application of quercetin in neurological disorders: from nutrition to nanomedicine. *Rev. Neurosci.* **2019**, *30*, 555–572.
- (65) Zamani, A.; Xiao, J.; Turnley, A. M.; Murray, S. S. Tropomyosin-Related Kinase B (TrkB) Regulates Neurite Outgrowth via a Novel Interaction with Suppressor of Cytokine Signalling 2 (SOCS2). *Mol. Neurobiol.* **2019**, *56*, 1262–1275.
- (66) Hu, Y.; Cho, S.; Goldberg, J. L. Neurotrophic effect of a novel TrkB agonist on retinal ganglion cells. *Invest. Ophthalmol. Visual Sci.* **2010**, *51*, 1747–1754.
- (67) Kaech, S.; Banker, G. Culturing hippocampal neurons. *Nat. Protoc.* **2006**, *1*, 2406–2415.

(68) Ferreira, T. A.; Blackman, A. V.; Oyrer, J.; Jayabal, S.; Chung, A. J.; Watt, A. J.; Sjöström, P. J.; van Meyel, D. J. Neuronal morphometry directly from bitmap images. *Nat. Methods* **2014**, *11*, 982–984.